



**HAL**  
open science

## Building efficient biocathodes with *Acidithiobacillus ferrooxidans* for the high current generation

Ganesan Sathiyarayanan, Nicolas Chabert, Joris Tulumello, Wafa Achouak

### ► To cite this version:

Ganesan Sathiyarayanan, Nicolas Chabert, Joris Tulumello, Wafa Achouak. Building efficient biocathodes with *Acidithiobacillus ferrooxidans* for the high current generation. *Journal of Power Sources*, 2021, 514, pp.230586. 10.1016/j.jpowsour.2021.230586 . cea-03534674

**HAL Id: cea-03534674**

**<https://cea.hal.science/cea-03534674v1>**

Submitted on 16 Oct 2023

**HAL** is a multi-disciplinary open access archive for the deposit and dissemination of scientific research documents, whether they are published or not. The documents may come from teaching and research institutions in France or abroad, or from public or private research centers.

L'archive ouverte pluridisciplinaire **HAL**, est destinée au dépôt et à la diffusion de documents scientifiques de niveau recherche, publiés ou non, émanant des établissements d'enseignement et de recherche français ou étrangers, des laboratoires publics ou privés.



Distributed under a Creative Commons Attribution - NonCommercial 4.0 International License

## **Building efficient biocathodes with *Acidithiobacillus ferrooxidans* for the high current generation**

**Ganesan Sathiyarayanan<sup>1\*</sup>, Nicolas Chabert<sup>1,2</sup>, Joris Tulumello<sup>1,2</sup>, Wafa Achouak<sup>1,3\*</sup>**

<sup>1</sup> *Laboratory of Microbial Ecology of the Rhizosphere & Extreme Environment (LEMIRE), BIAM, CEA Cadarache, 13108 Saint Paul-lez-Durance, France.*

<sup>2</sup> *BioIntrant, 139 Rue Philippe de Girard, 84120 Pertuis, France.*

<sup>3</sup> *Aix Marseille University, CNRS, FR 3098 ECCOREV, 13545 Aix-en-Provence, France.*

*\*Corresponding authors.*

*E-mail addresses:* sathiyamicrog@gmail.com (G. Sathiyarayanan); wafa.achouak@cea.fr (W. Achouak)

## Abstract

The development of biocathodes is highly fascinating in microbial electrochemical technologies research. In this study, iron-oxidizing bacterium *Acidithiobacillus ferrooxidans*-based biocathodes were developed under the constant polarization of the electrochemical reactors at  $-0.2\text{ V vs. Ag/AgCl}$  with a pH of 2. On the 15<sup>th</sup> day of the 21-day batch experiment, *A. ferrooxidans*-based biocathode produced a maximum current density of  $-38.61 \pm 13.16\text{ A m}^{-2}$  when the reactors were supplemented with 125 mM  $\text{Fe}^{2+}$  ions as an electron donor and 9 mM citrate as an iron chelator to buffer the iron-rich medium. Oxidation of  $\text{Fe}^{2+}$  to  $\text{Fe}^{3+}$  by *A. ferrooxidans* and its electrochemical regeneration at the cathode were mainly responsible for the high current generation. Furthermore, in the presence of iron, *A. ferrooxidans* develop a multi-layer biofilm on the cathode surface, which could potentially perform an indirect electron transfer mechanism.

**Keywords:** Biocathode, *Acidithiobacillus ferrooxidans*, Biofilm, Current density, Indirect electron transfer

## 1. Introduction

Microbial fuel cell (MFC) is a promising bio-electrochemical system that converts chemical energy to electrical energy using extracellular electron transferring microorganisms as biocatalysts [1]. Currently, MFC and other microbial electrochemical technologies (METs) are still in infancy due to the low current/power outputs [2,3] and limited oxygen reduction reaction (ORR) kinetics at the abiotic cathode [4]. Metal-based catalysts (i.e., platinum, ruthenium, iridium, etc.) are often used to enhance the ORR at the abiotic cathode chamber [4]; however, the kinetics of the ORR is slow and coupled with high overpotentials. Platinum-based catalysts are also increasing the cost, which limits the operational sustainability of MFCs [5]. Most recently, alternative cathode reactions emerged instead of ORR using redox shuttles as an electron transfer mediator (e.g.  $\text{Fe}^{2+}/\text{Fe}^{3+}$ ,  $\text{Mn}^{2+}/\text{MnO}_2$ ,  $\text{Mn}^{2+}/\text{Mn}^{3+}$ ,  $\text{Co}^{2+}/\text{Co}^{3+}$  etc.) [5]. Such alternative reaction at the cathode chamber along with biological catalyst (i.e., electrotrophic bacteria) [3] resulted in a higher cathode potential than is typically achieved with ORR on platinum-based catalysts in MFCs [6,7]. Especially, MFC systems developed with *Acidithiobacillus ferrooxidans* showed the reduction of  $\text{Fe}^{3+}$  irons and subsequent biological oxidation at the cathode with an improved current generation [6,8]. *A. ferrooxidans* (formerly known as *Thiobacillus ferrooxidans*) is a chemolithoautotrophic and obligate acidophilic bacterium that thrives at extremely low pH (1 to 3.5, optimum ~2.0). This bacterium obtains energy by oxidizing the  $\text{Fe}^{2+}$  to  $\text{Fe}^{3+}$  ions and utilizing molecular oxygen as a terminal electron acceptor. Reduced sulfur ( $\text{S}^{\text{red}}$ ), elemental sulfur ( $\text{S}^0$ ), and hydrogen ( $\text{H}_2$ ) can also act as electron donors in certain cases [9,10]. The energy obtained from the oxidation of iron or sulfur is used to fix the  $\text{CO}_2$  from the atmosphere by Calvin–Benson–Bassham cycle [9]. The iron-oxidizing potential is widely used to extract metals from ores, especially in acid mines and *A. ferrooxidans* also plays a vital role in metal biogeochemical cycling in acid environments [10].

*A. ferrooxidans* exhibits electrolithoautotrophy, which can use electrons from a polarized electrode to develop biocathode even at the extreme acidic pH [11].  $\text{Fe}^{2+}$  ions can act as an efficient electron donor and mediator to enhance the *A. ferrooxidans*-based biocathode development and current generation [12,13]. In *A. ferrooxidans*, iron-based metabolism results in a higher current density than sulfur-based metabolism [14]; however, the impact of the  $\text{Fe}^{2+}$  ions concentration on the current generation is unknown. Furthermore, iron can stimulate the synthesis of the outer membrane cytochrome proteins (Cyc2) in *A. ferrooxidans* [14] by activating the direct electron transfer mechanism [15]. The electrochemical cultivation of *A. ferrooxidans* showed the bacterial oxidation of  $\text{Fe}^{2+}$  and

electrochemical regeneration at the cathode through the iron redox cycling process [13,16]. Usually, *A. ferrooxidans* grow slowly under the standard iron-rich cultivation method due to the inhibitory effect of surplus  $\text{Fe}^{2+}$  ions and the formation of  $\text{Fe}^{3+}$  precipitates in the growth medium [17]. Iron chelator such as citrate has been used to buffer the  $\text{Fe}^{2+}$  rich medium to reduce the precipitation [18] and enhance the electrochemical processing of *A. ferrooxidans* [19].

*A. ferrooxidans* have been tested as a cathode catalyst in MFCs, where the bioanodes enriched with exoelectrogenic microbial communities [6,8,13,20] produced a maximum current density of  $4.4 \text{ A m}^{-2}$ . However, bio-cathodes solely developed with *A. ferrooxidans* (pure culture) as a cathode bio-catalyst showed the highest current density of  $5 \text{ A m}^{-2}$ , where graphite felt was used as a working electrode with an  $11.8 \text{ cm}^2$  projected area [11]. Therefore, further optimization of *A. ferrooxidans*-based biocathodes will open doors to achieving high current densities [11]. To meet this challenge, we have systematically optimized bioelectrochemical experiments by investigating the impact of the mediator ( $\text{Fe}^{2+}$  ions), iron chelator (citrate ions), and applied potential on electrochemical processing of *A. ferrooxidans* for the high current generation. As a result, highly improved biocathodes were developed under constant polarization using a three-electrode reactor system to precisely characterize the kinetics and intrinsic properties of the working electrode while avoiding most of the possible interactions that occur in typical MFC. Furthermore, the growth of the biofilm on the cathode surface (i.e., biocathode) was confirmed by confocal laser scanning microscopy (CLSM).

## 2. Materials and Methods

### 2.1. Microorganism and culture conditions

*A. ferrooxidans* ATCC 23270<sup>T</sup> was kindly offered by Dr. Violaine Bonnefoy (Laboratory of Bacterial Chemistry, CNRS/Aix-Marseille University, France) and used throughout the study. The bacterial strain was regularly grown in ATCC 2436 9K medium comprised of two different solutions, in which solution 1 includes  $3.0 \text{ g l}^{-1} (\text{NH}_4)_2\text{SO}_4$ ,  $0.5 \text{ g l}^{-1} \text{ MgSO}_4 \cdot 7\text{H}_2\text{O}$ ,  $0.5 \text{ g l}^{-1} \text{ K}_2\text{HPO}_4$ ,  $0.1 \text{ g l}^{-1} \text{ KCl}$ ,  $0.01 \text{ g l}^{-1} \text{ Ca}(\text{NO}_3)_2$  in 700 ml of deionized water. The pH of solution 1 was customized to 5.5 with  $\text{H}_2\text{SO}_4$  and autoclaved. Solution 2 was composed of  $44.22 \text{ g l}^{-1} \text{ FeSO}_4 \cdot 7\text{H}_2\text{O}$  in 300 ml of deionized water, and the pH was customized to 1.4 with  $\text{H}_2\text{SO}_4$  and sterilized by filtration ( $0.2 \mu\text{m}$  filters, Thermo Scientific, Waltham, MA). Both solutions 1 and 2 were mixed under a sterile environment and dispensed (50 ml) into 250 ml clean screw cap shake flasks. The final pH of the medium would be  $\sim 2$  while combining both solutions 1 and 2, and pH 2 is optimum for the growth of

*A. ferrooxidans* [9,10]. 9K medium was inoculated with previously grown log-phase *A. ferrooxidans* culture (2%), which provides the initial bacterial cell concentration of  $\approx 10^6$  cells  $\text{ml}^{-1}$ . Inoculated flasks were maintained under a shaking incubator (150 RPM) at 30 °C for a week. Similarly, log-phase cells were maintained by weekly subculture into fresh media. All chemicals were from Sigma–Aldrich (St. Louis, MO) unless otherwise mentioned.

## **2.2. Bioelectrochemical experiments**

### **2.2.1. Reactors**

A three-electrode system was used for all electrochemical experiments, which comprises the working (here, i.e., cathode), counter, and reference electrode. DURAN™ GL45 laboratory glass bottles (DWK Life Sciences, Germany) were used to construct the reactors with a total capacity of 250 ml, 70 mm diameter, and 143 mm height. Reactors were closed with 35–45 mm inner diameter plastic foam plugs, which prevent contamination, and the electrodes can be quickly introduced into the reactor through these plugs. A rectangular piece of carbon cloth-based gas diffusion electrode (GDE) with the macroporous surface was used as the working electrode (i.e., cathode) with an area of 3  $\text{cm}^2$  (1 cm  $\times$  3 cm), a thickness of 356  $\mu\text{m}$ , and the characteristic mass of around 0.05 g (PaxiTech SAS, Echirolles, France). A piece of RVG4000 graphite felt having an area of about 12  $\text{cm}^2$  (3 cm  $\times$  4 cm) with a thickness of 12 mm (Mersen, Gennevilliers, France) was used as the counter electrode (auxiliary). Ag/AgCl (sat. KCl) electrode with 110 mm height and 12 mm diameter (Sigma-Aldrich, Inc) was used as the reference electrode ( $E^\circ = 0.197$  V). The reference electrode was washed with 70% (vol/vol) ethanol and further sterilized by UV for 30 minutes. The current collector, such as titanium wires (1.5 mm diameter) (Goodfellow Cambridge Ltd, England), were weaved separately through the working and counter electrode and extended through the foam plugs passage of the reactor cap. The reactor system with the working and counter electrode was sterilized by autoclaving. A three-electrode reactor system used in this study is shown in Fig. S1, and the reactor setup under the laboratory environment is shown in Fig. S2.

### **2.2.2. electrolyte and inoculation of reactors**

Electrochemical experiments were performed using ATCC 2436 9K medium as an electrolyte in the presence (15 mM  $\text{Fe}^{2+}$ ) and absence of  $\text{Fe}^{2+}$  ions. 9K medium was prepared as described in section 2.1, except solution 2 was slightly modified with 15 mM  $\text{Fe}^{2+}$  ions. The solution 1 and 2 were adjusted to pH 2.0 using  $\text{H}_2\text{SO}_4$  and sterilized separately by autoclaving at 121 °C for 30 min and filtered through 0.2  $\mu\text{m}$  Whatman® filter papers (Sigma-Aldrich, Inc), respectively. Both solutions were mixed under aseptic conditions, and about 200 ml of 9K medium was dispensed into a sterile reactor setup that was already equipped

with a working and counter electrode. Also, UV sterilized Ag/AgCl reference electrode was inserted into the reactor setup through foam plugs. The log-phase *A. ferrooxidans* cells were washed twice with sterile water at 1000×g for 5 minutes, and reactors were inoculated about the initial cell concentration of  $\approx 10^6$  cells ml<sup>-1</sup>. Control experiments were performed using a similar three-electrode reactor setup without adding the *A. ferrooxidans* culture (abiotic).

### 2.2.3. Operation and electrochemical measurements

The reactors were maintained in a thermostatic water bath at 30 °C, and the electrodes were connected to 16 channel potentiostats equipped with EC-Lab software (MPG-2 or VMP3, BioLogic Science Instruments, France). The electrochemical reactors were operated in batch mode for 15 days, and some experiments were conducted for 21 days. The reactors were polarized at -0.2 V vs. Ag/AgCl through the chronoamperometry (CA) technique. The negative potential was used to prevent the abiotic formation of peroxide on carbon fiber and improve the possible energy production in bacteria [21]. In addition to that, *A. ferrooxidans* prefer the potential of -0.2 V to form biocathodes [12]. Current production (I) was measured (A m<sup>-2</sup>) continuously with 2-minute intervals. Cyclic Voltammetry (CV) was performed (-0.8 to 0.8 V vs. Ag/AgCl) at the end of the experiments with a scan rate of 5 mV s<sup>-1</sup> as previously described for electroactive biofilms [22]. Initial and intermittent CV disturbs the bacterial biofilm development [12,23,24]; hence CV was performed at the end of the experiments. In some CV experiments (15 mM Fe<sup>2+</sup>), O<sub>2</sub> and N<sub>2</sub> were bubbled into the electrolyte for at least 10 minutes to detect oxygen reduction. The potentials recorded vs. Ag/AgCl were normalized to the reversible hydrogen electrode (RHE) range using the Nernst equation:

$$E_{(\text{RHE})} = E_{\text{Ag}/\text{AgCl}} + 0.059 \cdot \text{pH} + E^{\circ}_{\text{Ag}/\text{AgCl}} \quad \text{Eq. 1}$$

where  $E_{(\text{RHE})}$  is the normalized potential vs. RHE,  $E_{\text{Ag}/\text{AgCl}}$  is the recorded potential vs. Ag/AgCl, and  $E^{\circ}_{\text{Ag}/\text{AgCl}}$  is the potential of Ag/AgCl (sat. KCl) at 25 °C (0.197 V). All of the potentials stated in this work are against RHE unless otherwise mentioned.

### 2.3. Electrochemical experiments with different concentrations of Fe<sup>2+</sup> ions

9K electrolyte medium (see section 2.1) with different concentrations of FeSO<sub>4</sub>·7H<sub>2</sub>O such as 25, 50, 100, 125, and 150 mM were prepared with pH 2.0. Three-electrode reactor systems were prepared, inoculated, and operated as described in section 2.2. The reactors were polarized at -0.2 V vs. Ag/AgCl (RE) for 15 days at 30 °C. The reactors inoculated with a pure culture of *A. ferrooxidans* were treated as biotic and were noted as abiotic control experiments without bacterial cells. Current density vs. time was recorded using the CA method, and the CV was performed at the end of experiments as previously stated in section 2.2.3.

#### **2.4. Electrochemical experiments with an iron chelator**

Trisodium citrate dihydrate ( $C_6H_5Na_3O_7 \cdot 2H_2O$ ) was used to buffer the iron-rich medium (9K) to **reduce**  $Fe^{3+}$  precipitation. First, 9K medium (pH 2.0) was prepared (see section 2.1) with 125 mM  $Fe^{2+}$  ions and 1 mM trisodium citrate (chelator) to **know the significance** of citrate on biocathode development and current generation. Secondly, 9K medium solution 1 was further simplified [ $0.4 \text{ g l}^{-1} (NH_4)_2SO_4$ ,  $0.4 \text{ g l}^{-1} MgSO_4 \cdot 7H_2O$ ,  $0.4 \text{ g l}^{-1} KH_2PO_4$ ,  $C_6H_5Na_3O_7 \cdot 2H_2O$  (0, 1, 3, and 9 mM)] [25] and designated as 9K1, where both solutions 1 and 2 (125 mM  $Fe^{2+}$ ) were adjusted to pH 2.0 with  $H_2SO_4$ . The citrate concentrations beyond 9 mM were not tested due to the interruption of electrochemical processes by excessive chelating reactions, which also affect the electrochemical regeneration of  $Fe^{2+}$  on the cathode. The reactors were prepared, inoculated, and operated as mentioned in section 2.2. Electrochemical reactors containing 9K and 9K1 medium were polarized at  $-0.2 \text{ V vs. Ag/AgCl}$  for 15 and 21 days, respectively. Current density vs. time **was recorded** continuously using **the CA method, and the CV was performed at the end of the experiments.**

#### **2.5. Electrochemical experiments with modified poise potential**

The reactors containing 9K1 medium (125 mM  $Fe^{2+}$  and 9 mM trisodium citrate) with pH 2.0 were polarized at  $0 \text{ V vs. Ag/AgCl}$ . Both biotic and abiotic reactors were operated for 21 days at  $30 \text{ }^\circ\text{C}$  to assess the impact of the poised potential on the biocathode development and current generation. **Current density vs. time was recorded continuously using the CA method, and CV analysis was performed** at the end of batch experiments.

#### **2.6. Total iron measurement and growth curve determination**

Residual concentration of  $Fe^{2+}$  and  $Fe^{3+}$  ions was measured by ferrozine-based assay [26]. After **completing electrochemical** experiments, the electrolyte samples were collected and filtered through Minisart<sup>®</sup>  $0.2 \text{ } \mu\text{m}$  filter unit (Sartorius Stedim Biotech, France) to remove the *A. ferrooxidans* cells. Briefly, 0.1% ferrozine (Sigma–Aldrich, St. Louis, MO) was mixed with an electrolyte sample. The magenta-colored complex was measured by Secomam PRIM spectrophotometer (Kisker Biotech GmbH & Co. KG, Germany) to quantify  $Fe^{2+}$  ions concentration. Total iron concentration was determined by using 10% hydroxylammonium acid to reduce all  $Fe^{3+}$  to  $Fe^{2+}$ .  $Fe^{3+}$  was then calculated from the difference between total Fe and  $Fe^{2+}$ . Bacterial planktonic growth was determined by bacterial cell count using a BX50

Olympus microscope at 400-fold magnification using a Neubauer-hemocytometer ( $0.02\text{mm} \times 0.025\text{mm}^2$ ).

### ***2.7. Confocal laser scanning microscopy (CLSM) for biofilm analysis***

The cathode biofilms were scanned by FluoView FV10i CLSM (Olympus) since it has been widely used for **studying electroactive bacteria, including mono or multi-layers** of biofilm on the electrode [12,27,28]. For CLSM scanning, the WE (cathode) were isolated from the reactors at the end of the experiments. About  $1\text{cm}^2$  of cathode electrode was sliced, and biofilms were stained with SYTO<sup>®</sup>9 (BacLight viability kit, Invitrogen) for 20 minutes. Further, SYTO<sup>®</sup>9 stained electrodes were rinsed **with filter-sterilized water** to remove planktonic cells (free-living cells) and then placed on a microscopic glass slide and enclosed with microscopic coverslips. Green fluorescent SYTO<sup>®</sup>9 tagged cells were imaged using excitation and emission wavelength at 473 nm and 510 nm, respectively. Carbon fibers in the electrodes were red-imaged using excitation and emission wavelength at 559 nm and 620 nm, respectively. Image (z) stacks were produced every  $1\text{ }\mu\text{m/slice}$  (sampling speed  $2.0\text{ }\mu\text{s/Pixel}$ ), and 3D projections were created using the FV10-ASW 4.1 software (Olympus), **especially to study the multi-layers of cathode biofilm. Three to five random fields per electrode for each experiment and at least three replicates were examined.** Initially, a global map of the biofilm was scanned under 10x ( $512 \times 512$  pixels,  $2.4\text{ }\mu\text{m/pixel}$ ), and a further 60x oil immersion objective ( $1,024 \times 1,024$  pixels,  $0.2\text{ }\mu\text{m/pixel}$ ) was used to elucidate the bacterial cell attachment on the carbon fiber in a high resolution. The bio-volume (average thickness) of the mono or multi-layer biofilms (10x map images,  $512 \times 512$  pixels,  $2.4\text{ }\mu\text{m/pixel}$ ) was analyzed using FV10-ASW 4.1 software (Olympus).

### ***2.8. Statistical analysis***

All biocathode experiments were performed in triplicate ( $n = 3$ ) for each condition. All primary data were presented as mean  $\pm$  standard deviation (SD), and the data were analyzed using Microsoft Excel 2016, R language, and Origin Pro 8.1 software.

## **3. Results and Discussion**

### ***3.1. Current generation in the absence and presence of $\text{Fe}^{2+}$ mediator***

Initial biocathode experiments were conducted in the absence and presence of a redox mediator ( $\text{Fe}^{2+}$ ). **In the absence of  $\text{Fe}^{2+}$  ions, *A. ferrooxidans* produced a maximum current density of  $-0.41 \pm 0.20\text{ A m}^{-2}$  on the 14<sup>th</sup> day of the chronoamperometric measurement (Fig.**

1a). A slow increase of current density due to the gradual development of biofilm on the electrode [11], where the applied potential ( $-0.2$  V) was the only source of electrons for their growth (electrolithoautotrophy). In contrast, adding a 15 mM concentration of  $\text{Fe}^{2+}$  ions as a mediator/electron donor resulted in exponential current generation within a day of experiment start-up. The maximum current density of  $-3.35 \pm 0.33$  A  $\text{m}^{-2}$  was recorded during the 4<sup>th</sup> day of the CA measurement. The sudden onset of the current generation is mainly due to the development of biocathodes where the electrolyte was amended with  $\text{Fe}^{2+}$  ions as an electron donor. The current generation became stable after 10 days of the bio-electrochemical process, and the current density sustained around  $-2.26 \pm 0.03$  A  $\text{m}^{-2}$  until the end of the batch experiment (Fig. 1a). Abiotic control experiments (without any bacterium) show negligible current density for similar experimental conditions (Fig. 1b and Table. S1).

Fig.1c and 1d show the CV curves of biotic and abiotic systems, respectively. The biotic system offers a sizeable integral area of CV curves when compared to the abiotic system in the presence of an iron source (15mM). Both (biotic and abiotic) systems show a comparatively smaller area CV loop without an iron source. In the 15mM iron source, the biotic system shows two firm reduction peaks at 0.42 V and  $-0.08$  V vs. RHE. The prominent reduction peak starts at 0.78 V as the onset potential and reaches the maximum current at 0.42 V, which strongly indicates the reduction of  $\text{Fe}^{3+}$  to  $\text{Fe}^{2+}$ . The onset potential (0.78 V) is close to the redox potential of the  $\text{Fe}^{3+}/\text{Fe}^{2+}$  pair (0.77 V), which agrees with the previously reported experimental models for electrochemical processing of *A. ferrooxidans* [29,30]. The oxidation of  $\text{Fe}^{2+}$  to  $\text{Fe}^{3+}$  ions was observed in the biotic reactors amended with 15 mM with an onset potential around 0.78 V. Biotic reactors had shown a second reduction peak with an onsite potential around  $-0.03$  V. It centered at  $-0.08$  V, which possibly reduction of  $\text{Fe}^{2+}$  iron to elemental form ( $\text{Fe}^{3+} + 3\text{e} \rightleftharpoons \text{Fe}$ ) [31]. In addition, the outer-membrane cytochrome c (Cyc2) might be responsible for the reduction peak at  $-0.08$  V since such reduction was not observed in the abiotic system (Fig. 1c). The overall CV analysis shows the substantial oxidation/reduction in the iron amended reactors, which confirm the existence of  $\text{Fe}^{2+}/\text{Fe}^{3+}$  redox couple in the biocathode system. In the absence of iron, *A. ferrooxidans* utilize the cathode electrons to perform ORR mediated by Fe species excreted by bacterial cells with a potential around 0.45V vs. SCE [11]. In this study, iron was used as a mediator (15 mM), and the CV analysis with and without oxygen experiments showed no apparent shift for the onset potential of the ORR. However, the presence of a pseudo-reversible signal around 0.75V, which corresponds to the  $\text{Fe}^{2+}/\text{Fe}^{3+}$  redox couple (Fig. S3). Also, there is not much difference between the CVs obtained with and without oxygen suggest the limited effect of oxygen on

the electrochemical reaction occurring at the cathode (Fig. S3). Thus, our results would substantiate a mediated electron transfer between the electrode and *A. ferrooxidans* cells [13]. In addition, in the presence of iron in the electrolyte (9K growth medium), there is no direct biological catalysis of the oxygen reduction at the electrode, despite molecular oxygen being utilized as the terminal electron acceptor by *A. ferrooxidans*.

CLSM z-stacks images of Fig. 1e and 1f show that biofilm was developed on the electrode by *A. ferrooxidans* in the absence and presence of  $\text{Fe}^{2+}$  with an average thickness of  $2\ \mu\text{m}$  and  $5\ \mu\text{m}$ , respectively. Especially, *A. ferrooxidans* had developed a monolayer biofilm on the carbon fibers in the absence of  $\text{Fe}^{2+}$  ions (Fig. 1g). Furthermore, in the presence of a 15 mM iron source, the same bacterium had formed multi-layer biofilm (Fig. 1h), which was identified through z-stack image analysis. Multilayer biofilm formation was critically confirmed by reconstructing the 3D image (z) stacks obtained every  $1\ \mu\text{m}/\text{slice}$  using CLSM. However, *A. ferrooxidans* monolayer biofilms [32] and its direct electron transfer mechanism through Cyc2 membrane protein have been reported in the literature to date [12,29]. Our results demonstrate that this bacterium can also develop multi-layer biofilms on the electrode surface in the presence of  $\text{Fe}^{2+}$  ions as an electron transfer mediator that notably increases the reduction current.

### 3.2. Effect of $\text{Fe}^{2+}$ ion concentration on current generation and cathodic biofilm development

Fig. 2a shows the significant increase in reduction current while increasing the initial concentration of the  $\text{Fe}^{2+}$  ions in the 9K medium. The maximum current about  $-3.86 \pm 1.89$ ,  $-7.85 \pm 4.13$ ,  $-15.55 \pm 5.46$ ,  $-24.37 \pm 2.58$ , and  $-19.42 \pm 8.87\ \text{A m}^{-2}$  were recorded from the biotic reactors with 25, 50, 100, 125, and 150 mM of  $\text{Fe}^{2+}$  ions, respectively (Table. S1). Like 15 mM  $\text{Fe}^{2+}$ , 25 mM  $\text{Fe}^{2+}$  ions containing reactors also suddenly reached the maximum current density due to bacteria's rapid consumption of available  $\text{Fe}^{2+}$  ions and subsequent biofilm development. After getting the maximum current, electrochemical reactors with 25, 50, 100, 125, and 150 mM of  $\text{Fe}^{2+}$  ions had shown the sustained current densities of  $-3.31 \pm 0.18$ ,  $-6.80 \pm 0.07$ ,  $-13.84 \pm 0.58$ ,  $-17.10 \pm 3.72$ ,  $-18.24 \pm 0.62\ \text{A m}^{-2}$ , respectively. Beyond 150 mM,  $\text{Fe}^{2+}$  ion concentrations were not tested since 100 mM of soluble iron is optimum for *A. ferrooxidans* cell growth per mole of  $\text{Fe}^{2+}$  ions [16].

Residual  $\text{Fe}^{2+}$  ion concentrations were measured to determine the  $\text{Fe}^{2+}$  oxidation potential ( $\text{Fe}^{2+}$  to  $\text{Fe}^{3+}$ ) of bacteria during the electrochemical growth, which indicates a substantial decrease in  $\text{Fe}^{2+}$  ion concentration. In contrast, in the abiotic systems,  $\text{Fe}^{2+}$  concentration was approximately stable (Table S2). It is likely that the first layer of the

biofilm directly oxidizes the *cathode via Cyc2*, while the upper layers may oxidize  $\text{Fe}^{2+}$  to promote their growth.  $\text{Fe}^{3+}$  could also be electrochemically reduced at the cathode surface and thus contribute to current production, probably with slower reaction rates concerning their diffusion kinetics [33,34]. Therefore, high current densities are mainly due to the bacterial oxidation of  $\text{Fe}^{2+}$  ions. In contrast, abiotic reactors had shown very low current densities with a similar trend (increasing from 25 to 150 mM) (Fig. 2b and Table S1). The abiotic current increases with time since the soluble  $\text{Fe}^{2+}$  and  $\text{Fe}^{3+}$  ions can be electrochemically oxidized or reduced on the electrode surface, especially oxidation at the anode and reduction at the cathode, even in the absence of bacteria [16].

In contrast, abiotic oxidation of  $\text{Fe}^{2+}$  was also evidenced by residual iron measurements (Table S2). Various factors may influence the abiotic oxido-reduction of iron, such as oxygen and modification of the electrode surface. Abiotic reactions were prolonged that reflects as low current generation than biotic experiments, in general. Fig. 2c shows the CV curves of the biotic system with different initial concentrations of  $\text{Fe}^{2+}$  ions. The electrochemical regeneration of  $\text{Fe}^{3+}$  was observed below 0.7 V vs. RHE in general. High iron concentration biocathodes (100, 125, and 150 mM) show a large integral area of CV curves compared to the low iron concentration systems (25 and 50 mM) in the presence of bacteria. Biocathodes developed with 25 and 50 mM of iron source show strong reduction peaks at 0.44 V and 0.40 V with onset potential about 0.79 V and 0.76 V, respectively, which confirms the reduction of  $\text{Fe}^{3+}$  to  $\text{Fe}^{2+}$ . Strong oxidization with an onset potential of 0.77 V indicates the oxidation of  $\text{Fe}^{2+}$  to  $\text{Fe}^{3+}$  ions. Therefore, 25 and 50 mM of soluble iron ( $\text{Fe}^{2+}$  and  $\text{Fe}^{3+}$ ) system had shown electrochemical redox reaction at the electrode surface. In contrast, 100, 125 and 150 mM  $\text{Fe}^{2+}$  ions had large reduction peak separation centered at 0.40, 0.36 and 0.29 V, respectively. These reduction peaks also had an onset potential around 0.76 V, confirming the reduction of  $\text{Fe}^{3+}$  to  $\text{Fe}^{2+}$ . In addition, the reduction current greatly increased, and the oxidation current decreased (Fig. 2c), proving that the  $\text{Fe}^{3+}$  concentration increased and  $\text{Fe}^{2+}$  concentration decreased due to bacterial oxidation of  $\text{Fe}^{2+}$ . The residual iron measurements also confirm this  $\text{Fe}^{2+}/\text{Fe}^{3+}$  fluctuation (Table S2). Besides, mid-point potentials of  $\text{Fe}^{2+}/\text{Fe}^{3+}$  had a variation with the standard potentials (0.77 V) [33], and it is prevalent in acidophilic bacteria that grow at extremely low pH [35].

Fig. 2 (d, e, f, g, and h), which shows CLSM images of the *A. ferrooxidans* biofilms developed on the cathode with 25, 50, 100, 125, and 150 mM  $\text{Fe}^{2+}$  ions, revealed the metabolically active biofilms with an average thickness of 6, 10, 17, 20, and 19  $\mu\text{m}$  respectively. Furthermore, 3D projection z-stack image analysis exhibits the multiple layers of

active cells, which obtain most of the energy from the oxidation of  $\text{Fe}^{2+}$  ions and the consumption of electrons from the poised potential ( $-0.2$  V). Active biofilms populated the carbon fibers, possibly performing the indirect electron transfer reaction (Fig. 2i, j, k, l, and m). With an increase in average thickness of biofilm, reduction reaction by *A. ferrooxidans* also significantly increased. Our results demonstrate that the high current density is directly proportional to biofilm growth (Fig. S4), which is also a major influencing factor for the oxidation/reduction of iron according to the residual iron measurement (Table S2). The CV and biofilm analysis strongly support the existence of an indirect electron transfer between the electrode and bacteria, which is mediated by the  $\text{Fe}^{2+}/\text{Fe}^{3+}$  redox couple [13]. A dark orange color iron precipitates were observed at the bottom of the reactors were amended with 100, 125, and 150 mM of the iron source. Also, electrodes were covered with a red-orange layer, which might be the deposition of iron oxides/hydroxides. Usually, precipitation of iron complicates the growth of *A. ferrooxidans* [17] and electrochemical reduction of  $\text{Fe}^{3+}$  to  $\text{Fe}^{2+}$  on the electrode [19].

### 3.3. Effect of iron chelator (citrate) concentration on current generation and cathodic biofilm development

Biocathode performance was improved while adding an iron chelator into 9K medium with 125 mM  $\text{Fe}^{2+}$ . 1 mM of citrate addition to 9K medium with pH 2.0 had shown the maximum current production of  $-19.32 \pm 3.16$  A  $\text{m}^{-2}$  within 10 days of the electrochemical process (Fig. S5a). CV analysis exhibits a reduction curve with an onset potential at 0.81 V and reaches the maximum reduction current at 0.19 V, confirming the reduction of  $\text{Fe}^{3+}$  to  $\text{Fe}^{2+}$  ions (Fig. S5b). A reduction peak that appears below 0.385 V might be due to the  $\text{Fe}^{3+}$ -citrate to  $\text{Fe}^{2+}$ -citrate reduction or Cyc1, which is mainly responsible for the downhill electron transfer in *A. ferrooxidans* [36,37]. The electrochemical reactors amended with citrate had shown low current generation than the reactors without citrate (Fig. 2a); however, the average thickness of biofilm ( $26 \mu\text{m}$ ) had slightly increased than in the absence of citrate experiment ( $20 \mu\text{m}$ ). Interestingly, the residual  $\text{Fe}^{2+}$  and  $\text{Fe}^{3+}$  ions concentration had also increased in 125 mM with 1 mM citrate than a citrate-free system in the biotic and abiotic condition (Table S2). Therefore, a consecutive electrochemical experiment with 9K1 medium (a more simplified form of 9K medium) was performed to understand the effect of the citrate concentration on the biocathode development and current production.

Fig. 3a shows a substantial increase in the current production while increasing the citrate concentration in the 9K1 medium with 125 mM  $\text{Fe}^{2+}$ . In the biotic condition, reactors with 0, 1, 3, and 9 mM of citrate concentration had shown the maximum current densities of

$-24.09 \pm 3.38$ ,  $-27.84 \pm 3.21$ ,  $-29.79 \pm 1.98$ , and  $-38.61 \pm 13.16$  A m<sup>-2</sup>, respectively. 9 mM citrate experiment had shown the maximum current during the 15.65 days of the 21-day batch experiment and sustained about  $-35.60 \pm 1.08$  A m<sup>-2</sup> until the end of the batch process. Thus, the current generation was steadily increased, which confirms the importance of citrate in the electrochemical processing of *A. ferrooxidans*. The abiotic reactors produced the lowest current densities simultaneously (Fig. 3b and Table S1).

Interestingly, the residual Fe<sup>2+</sup> ion concentration was increased, and Fe<sup>3+</sup> ion concentration decreased while increasing the citrate addition to the 9K1 medium (Table S2). In the absence of citrate (0 mM), the bacteria generally consume all the Fe<sup>2+</sup> in the medium. In the presence of 9 mM citrate, the residual Fe<sup>2+</sup> concentration had increased eightfold over the 0 mM citrate condition (Table S2). A slight increase in Fe<sup>2+</sup> concentration was also observed in the abiotic reactor systems, which confirms the effect of citrate to stabilize the solubility of iron in the growth medium. In general, iron precipitation was gradually decreased in both biotic and abiotic systems while increasing the citrate concentration in the 9K1 medium (data not shown). Citrate addition slows the auto-oxidation of iron due to the chelation of Fe<sup>3+</sup> ions by citrate, which solubilizes the insoluble form of Fe<sup>3+</sup> precipitates into soluble Fe<sup>3+</sup> ions [19]. Then it can be easily electrochemically reduced to Fe<sup>2+</sup> at the cathode [13,16,34]. Our study shows that the solubilization of Fe<sup>3+</sup> is a dominant process than precipitation while adding citrate as a chelator to stabilize the electrochemical process. Therefore, the residual iron concentration (Fe<sup>2+</sup> and Fe<sup>3+</sup>) is relatively higher in citrate amended iron-rich medium than citrate-free medium. Moreover, citrate is non-toxic to *A. ferrooxidans* and does not interfere with bacterial iron oxidation [18].

CV analysis of biocathodes shows the possible electrochemical reactions occurring in the presence of citrate as a chelator (Fig. 3c). Biocathodes with 0, 1, 3, and 9 mM of citrate had shown an onset potential around 0.78 V, reached the maximum reduction current density at 0.0, 0.08, 0.17, and 0.03 V, respectively. This onset potential is directly related to the reduction of Fe<sup>3+</sup> to Fe<sup>2+</sup> [33]. Biocathode with 9 mM citrate had shown a slight hump at 0.355 V during the reverse scan of CV, which might be linked to Fe<sup>3+</sup>-citrate/Fe<sup>2+</sup>-citrate redox couple (0.37 V) [38]. Hence, electrochemical regeneration of Fe<sup>2+</sup> at the surface of the electrode shows the importance of citrate. The CLSM image analysis also substantiates the positive effect of citrate on the growth of *A. ferrooxidans* biofilm on the cathode surface (Fig. 3d, e, f, and g). Multilayer of biofilm was identified on the cathode with an average thickness of 17, 22, 25, and 30  $\mu$ m from the 0, 1, 3, and 9 mM of citrate amended reactors, respectively. The growth of bacteria on the carbon fibers provides clear evidence for biocathode

development (Fig. 3h, i, j, and k). The average thickness of biofilms and reduction current densities had increased while increasing the citrate addition. Therefore, increased solubility of  $\text{Fe}^{3+}$  plays a significant role in the enhanced current production by *A. ferrooxidans*.

### 3.4. Planktonic lifestyle and impact of applied potential on the current generation by *A. ferrooxidans*

*A. ferrooxidans* was further studied under electrochemical cultivation to understand the growth of bacteria in the planktonic state (free-living),  $\text{Fe}^{2+}/\text{Fe}^{3+}$  redox reaction, and the current production pattern (Fig. 4). The planktonic bacterial growth was gradually increased. At the same time, the initial  $\text{Fe}^{2+}$  concentration was decreased due to the bacterial oxidation of  $\text{Fe}^{2+}$ . The bacterial growth curve had reached the stationary phase on the 15<sup>th</sup> day of the process. The current generation also stabilized, suggesting that a planktonic lifestyle could promote the current output in *A. ferrooxidans*. The reduction current continued even near depletion of  $\text{Fe}^{2+}$  in the reactors, wherein the negative poised potential ( $-0.2$  V) only acts as an energy source for the bacterial growth and current production, which substantiates the importance of negative poised potential for the development of *A. ferrooxidans*-based biocathodes [12]. A further experiment was conducted with the potential of 0 V while maintaining the same reactor condition (125 mM  $\text{Fe}^{2+}$  and 9 mM citrate) to know the impact of  $-0.2$  V vs. Ag/AgCl on the current generation. The reactors polarized at 0 V had shown a maximum current density of  $-22.63 \pm 2.85$  A  $\text{m}^{-2}$  on the 15<sup>th</sup> day (Fig. S6a), which was significantly lesser than the original condition with poised potential ( $-0.2$  V vs. Ag/AgCl) (Table S1). The electrochemical regeneration of  $\text{Fe}^{2+}$  from  $\text{Fe}^{3+}$  is more or less similar, with an onset potential at 0.79 V (Fig. S6b). However, the biofilm's average thickness (20  $\mu\text{m}$ ) is lesser than the poised potential condition ( $-0.2$  V). As a result, the applied potential, especially negative potential, plays a vital role in developing biocathodes and generating the reduction current by *A. ferrooxidans*.

### 3.5 Possible electron transfer mechanisms in *A. ferrooxidans*

*A. ferrooxidans* can develop a mono and multi-layer biofilm in the absence and presence of iron, respectively. In addition, CV analysis also substantiates the oxidation-reduction occurring at the cathode. These remarks suggest a mediated electron transfer between the electrode and the bacteria. In the citrate-free experiments, the working electrodes were entirely covered with a red-orange layer of iron oxide/hydroxide deposition, which confirms the critical role of iron as a mediator for electron transfer. In the absence of iron, the

bacteria can perform the direct extracellular electron transfer involving a *c*-type cytochrome (Cyc2) [15,29], which allows electron uptake from the cathode for growth (electroautotrophy) [11]. Cytochrome-based direct electron transfer has already been proved in *A. ferrooxidans* [14,39,40]; however, indirect electron transfer mediated by redox shuttles remains unknown. CV analysis confirms the high concentration of Fe<sup>3+</sup> ions (due to the bacterial oxidation), also provides solid evidence for the electrochemical reduction of Fe<sup>3+</sup> to Fe<sup>2+</sup> on the electrode with an onset potential around 0.77 V, wherein the cathode potential is close to the reduction potential of Fe<sup>3+</sup> into Fe<sup>2+</sup>. Our results corroborate those of Izadi et al. [13], where similar electrochemical experiments were conducted with iron-oxidizing bacteria and suggested a predominantly Fe<sup>2+</sup>-mediated electron transfer mechanism. Electrochemical and bioenergetic studies on *A. ferrooxidans* also strongly suggest an indirect electron transfer mechanism between the electrode and bacterial Cyc2, where Fe<sup>2+</sup>/Fe<sup>3+</sup> redox shuttle is the mediator [6,8,13,29,34,36]. Our systematic biofilm analysis, CVs, and residual iron measurements also support the presence of an indirect electron transfer in *A. ferrooxidans*. Therefore, *A. ferrooxidans* might have both direct and indirect electron transfer mechanisms, as shown in Fig. 5, however, which needs further validation using Cyc2 mutant strains. This indirect electron transfer process can be executed by either planktonic or sessile (electrode attached) bacteria. Presumably, both mechanisms can co-exist if permitted by the reactor conditions, wherein soluble iron is likely acting as a redox shuttle [13].

Overall, the redox potentials discussed in this study (0 to 1 V) correspond to Fe<sup>2+</sup> to Fe<sup>3+</sup>-mediated downhill electron transfer that usually occurs in *A. ferrooxidans* [33]. Therefore, the high generation is mainly due to the Fe<sup>2+</sup>/Fe<sup>3+</sup> redox shuttle, as shown in Fig. 5. The reduction current generated here is higher than the previously reported *A. ferrooxidans*-based biocathodes and pure culture studies of electrotrophic microorganisms in general (Table 1). Due to differences between the bacterial strains and operating conditions, the current production is significantly varied from one biocathode to another. However, sustained current densities obtained from this study were highly promising than other electrotrophic biocathodes.

#### 4. Conclusions

Efficient biocathodes were developed with *A. ferrooxidans*, which produced a maximum current density of  $-38.61 \pm 13.16$  A m<sup>-2</sup>. The high current generation is due to oxidation of Fe<sup>2+</sup> to Fe<sup>3+</sup> by *A. ferrooxidans* and subsequent electrochemical reduction of Fe<sup>3+</sup> to Fe<sup>2+</sup> at the cathode, highlighting the importance of alternative cathode reactions with

mediators instead of routine ORR. The formation of multi-layer biofilm on the electrode was critically confirmed by CLSM analysis. Also, biofilm formation and increased solubility of  $\text{Fe}^{3+}$  are major influencing factors for the oxidation/reduction of iron at the cathode. Aside from the expected direct electron transfer, CV analysis and multi-layer biofilm formation strongly suggest the existence of an indirect electron transfer mechanism in *A. ferrooxidans*. Current densities obtained from this study were highly promising compared to the previously established pure culture-based biocathode studies. *A. ferrooxidans*-based biocathodes will be further studied with bioanodes in full-scale MFC systems to improve bioelectricity production.

### **CRedit authorship contribution statement**

**G. Sathiyarayanan:** Conceptualization, Methodology, Formal analysis, Validation, Visualization, Writing - original draft, Writing - review & editing. **N. Chabert:** Methodology, Writing - review & editing. **J. Tulumello:** Formal analysis, Visualization. **W. Achouak:** Project administration, Conceptualization, Supervision, Funding acquisition, Writing - review & editing.

### **Declaration of competing interest**

The authors declare that they have no known competing financial interests or personal relationships that could have influenced the work reported in this paper.

### **Acknowledgments**

This research was funded by CEA Enhanced Eurotalents fellowship (FP7 Marie Skłodowska-Curie COFUND Programme) and Excellence Initiative of Aix-Marseille University - A\*MIDEX, a French “Investissements d’Avenir” program, through its associated Labex SERENADE project. The authors would like to thank Dr. Suresh Kannan Balasingam (NTNU, Trondheim, Norway) for the critical reading of the manuscript and valuable suggestions about iron electrochemistry. The authors also thank Dr. Violaine Bonnefoy (LCB, IMM Marseille) for a fruitful discussion on the physiology and growth of *A. ferrooxidans*.

### **References**

- [1] A.J. Slate, K.A. Whitehead, D.A.C. Brownson, C.E. Banks, Microbial fuel cells: An overview of current technology, *Renew. Sust. Energ. Rev.* 101 (2019) 60–81.
- [2] B.E. Logan, K. Rabaey, Conversion of Wastes into Bioelectricity and Chemicals by Using

- Microbial Electrochemical Technologies, *Science* (80-. ). 337 (2012) 686–690.
- [3] B.E. Logan, R. Rossi, A. Ragab, P.E. Saikaly, Electroactive microorganisms in bioelectrochemical systems, *Nat. Rev. Microbiol.* 17 (2019) 307–319.
- [4] H. Yuan, Y. Hou, I.M. Abu-Reesh, J. Chen, Z. He, Oxygen reduction reaction catalysts used in microbial fuel cells for energy-efficient wastewater treatment: a review, *Mater. Horiz.* 3 (2016) 382–401.
- [5] H. Rismani-Yazdi, S.M. Carver, A.D. Christy, O.H. Tuovinen, Cathodic limitations in microbial fuel cells: An overview, *J. Power Sources.* 180 (2008) 683–694.
- [6] A. Ter Heijne, H.V.M. Hamelers, C.J.N. Buisman, Microbial Fuel Cell Operation with Continuous Biological Ferrous Iron Oxidation of the Catholyte, *Environ. Sci. Technol.* 41 (2007) 4130–4134.
- [7] A. Rhoads, H. Beyenal, Z. Lewandowski, Microbial Fuel Cell using Anaerobic Respiration as an Anodic Reaction and Biomineralized Manganese as a Cathodic Reactant, *Environ. Sci. Technol.* 39 (2005) 4666–4671.
- [8] A. Ter Heijne, H.V.M. Hamelers, V. de Wilde, R.A. Rozendal, C.J.N. Buisman, A Bipolar Membrane Combined with Ferric Iron Reduction as an Efficient Cathode System in Microbial Fuel Cells, *Environ. Sci. Technol.* 40 (2006) 5200–5205.
- [9] R. Quatrini, D.B. Johnson, *Acidithiobacillus ferrooxidans*, *Trends Microbiol.* 27 (2019) 282–283.
- [10] S. Zhang, L. Yan, W. Xing, P. Chen, Y. Zhang, W. Wang, *Acidithiobacillus ferrooxidans* and its potential application, *Extremophiles.* 22 (2018) 563–579.
- [11] S. Carbajosa, M. Malki, R. Caillard, M.F. Lopez, F.J. Palomares, J.A. Martín-Gago, N. Rodríguez, R. Amils, V.M. Fernández, A.L. De Lacey, Electrochemical growth of *Acidithiobacillus ferrooxidans* on a graphite electrode for obtaining a biocathode for direct electrocatalytic reduction of oxygen, *Biosens. Bioelectron.* 26 (2010) 877–880.
- [12] N. Chabert, V. Bonnefoy, W. Achouak, Quorum sensing improves current output with *Acidithiobacillus ferrooxidans*, *Microb. Biotechnol.* 11 (2018) 136–140.
- [13] P. Izadi, J.-M. Fontmorin, L.F.L. Fernández, S. Cheng, I. Head, E.H. Yu, High Performing Gas Diffusion Biocathode for Microbial Fuel Cells Using Acidophilic Iron Oxidizing Bacteria, *Front. Energy Res.* 7 (2019).
- [14] A. Yarzabal, G. Brasseur, J. Ratouchniak, K. Lund, D. Lemesle-Meunier, J.A. DeMoss, V. Bonnefoy, The High-Molecular-Weight Cytochrome *Cyc2* of *Acidithiobacillus ferrooxidans* Is an Outer Membrane Protein, *J. Bacteriol.* 184 (2002) 313–317.
- [15] M. Rosenbaum, F. Aulenta, M. Villano, L.T. Angenent, Cathodes as electron donors for microbial metabolism: Which extracellular electron transfer mechanisms are involved?, *Bioresour. Technol.* 102 (2011) 324–333.
- [16] S. Nakasono, N. Matsumoto, H. Saiki, Electrochemical cultivation of *Thiobacillus*

- ferrooxidans* by potential control, *Bioelectrochem. Bioenerg.* 43 (1997) 61–66.
- [17] J. Daoud, D. Karamanev, Formation of jarosite during Fe<sup>2+</sup> oxidation by *Acidithiobacillus ferrooxidans*, *Miner. Eng.* 19 (2006) 960–967.
- [18] X. Li, R. Mercado, T. Kernan, A.C. West, S. Banta, Addition of citrate to *Acidithiobacillus ferrooxidans* cultures enables precipitate-free growth at elevated pH and reduces ferric inhibition, *Biotechnol. Bioeng.* 111 (2014) 1940–1948.
- [19] X. Li, R. Mercado, S. Berlinger, S. Banta, A.C. West, Engineering *Acidithiobacillus ferrooxidans* growth media for enhanced electrochemical processing, *AIChE J.* 60 (2014) 4008–4013.
- [20] A. Ter Heijne, F. Liu, L.S. van Rijnsoever, M. Saakes, H.V.M. Hamelers, C.J.N. Buisman, Performance of a scaled-up Microbial Fuel Cell with iron reduction as the cathode reaction, *J. Power Sources.* 196 (2011) 7572–7577.
- [21] E.M. Milner, D. Popescu, T. Curtis, I.M. Head, K. Scott, E.H. Yu, Microbial fuel cells with highly active aerobic biocathodes, *J. Power Sources.* 324 (2016) 8–16.
- [22] E.M. Milner, E.H. Yu, The Effect of Oxygen Mass Transfer on Aerobic Biocathode Performance, Biofilm Growth and Distribution in Microbial Fuel Cells, *Fuel Cells.* 18 (2018) 4–12.
- [23] N. Chabert, O. Amin Ali, W. Achouak, All ecosystems potentially host electrogenic bacteria, *Bioelectrochemistry.* 106 (2015) 88–96.
- [24] M. Rimboud, M. Barakat, W. Achouak, A. Bergel, M.-L. Délia, Oxygen-reducing microbial cathodes in hypersaline electrolyte, *Bioresour. Technol.* (2020) 124165.
- [25] A. Yarzabal, K. Duquesne, V. Bonnefoy, Rusticyanin gene expression of *Acidithiobacillus ferrooxidans* ATCC 33020 in sulfur- and in ferrous iron media, *Hydrometallurgy.* 71 (2003) 107–114.
- [26] E. Viollier, P.W. Inglett, K. Hunter, A.N. Roychoudhury, P. Van Cappellen, The ferrozine method revisited: Fe(II)/Fe(III) determination in natural waters, *Appl. Geochemistry.* 15 (2000) 785–790.
- [27] M. Rimboud, W. Achouak, Electroautotrophy of *Thioalkalivibrio nitratireducens*, *Bioelectrochemistry.* 126 (2019) 48–55.
- [28] M. Rimboud, A. Bergel, B. Erable, Multiple electron transfer systems in oxygen reducing biocathodes revealed by different conditions of aeration/agitation, *Bioelectrochemistry.* 110 (2016) 46–51.
- [29] T. Ishii, S. Kawaichi, H. Nakagawa, K. Hashimoto, R. Nakamura, From chemolithoautotrophs to electrolithoautotrophs: CO<sub>2</sub> fixation by Fe(II)-oxidizing bacteria coupled with direct uptake of electrons from solid electron sources, *Front. Microbiol.* 6 (2015) 1–9.
- [30] T. Ishii, H. Nakagawa, K. Hashimoto, R. Nakamura, *Acidithiobacillus ferrooxidans* as a Bioelectrocatalyst for Conversion of Atmospheric CO<sub>2</sub> into Extracellular Pyruvic Acid,

- Electrochemistry. 80 (2012) 327–329.
- [31] D.R. Lide, CRC Handbook of Chemistry and Physics: A Ready-reference Book of Chemical and Physical Data, CRC-Press, 1995.
- [32] F. Crundwell, The formation of biofilms of iron-oxidising bacteria on pyrite, *Miner. Eng.* 9 (1996) 1081–1089.
- [33] W.J. Ingledew, *Thiobacillus Ferrooxidans* the bioenergetics of an acidophilic chemolithotroph, *Biochim Biophys Acta Rev Bioenerg.* 683 (1982) 89–117.
- [34] H.P. Bennetto, D.K. Ewart, A.M. Nobar, I. Sanderson, Microbial Fuel Cell Studies of Iron-Oxidising Bacteria, in: M.J. Allen, S.F. Cleary, F.M. Hawkrige (Eds.), *Charg. F. Eff. Biosyst.*, Springer US, Boston, MA, 1989: pp. 339–349.
- [35] D.B. Johnson, T. Kanao, S. Hedrich, Redox Transformations of Iron at Extremely Low pH: Fundamental and Applied Aspects, *Front. Microbiol.* 3 (2012).
- [36] L.J. Bird, V. Bonnefoy, D.K. Newman, Bioenergetic challenges of microbial iron metabolisms, *Trends Microbiol.* 19 (2011) 330–340.
- [37] C. Cavazza, M.T. Giudici-Ortoni, W. Nitschke, C. Appia, V. Bonnefoy, M. Bruschi, Characterisation of a soluble cytochrome c4 isolated from *Thiobacillus ferrooxidans*, *Eur. J. Biochem.* 242 (1996) 308–314.
- [38] B. Thamdrup, Bacterial Manganese and Iron Reduction in Aquatic Sediments, in: B. Schink (Ed.), *Adv. Microb. Ecol.*, Springer US, Boston, MA, 2000: pp. 41–84.
- [39] C. Castelle, M. Guiral, G. Malarte, F. Ledgham, G. Leroy, M. Brugna, M.-T. Giudici-Ortoni, A new iron-oxidizing/O<sub>2</sub>-reducing supercomplex spanning both inner and outer membranes, isolated from the extreme acidophile *Acidithiobacillus ferrooxidans*, *J. Biol. Chem.* 283 (2008) 25803–25811.
- [40] X. Wang, M. Roger, R. Clément, S. Lecomte, F. Biaso, L.A. Abriata, P. Mansuelle, I. Mazurenko, M.T. Giudici-Ortoni, E. Lojou, M. Ilbert, Electron transfer in an acidophilic bacterium: interaction between a diheme cytochrome and a cupredoxin, *Chem. Sci.* 9 (2018) 4879–4891.
- [41] T. de Campos Rodrigues, M.A. Rosenbaum, Microbial Electroreduction: Screening for New Cathodic Biocatalysts, *ChemElectroChem.* 1 (2014) 1916–1922.
- [42] S. Debuy, S. Pecastaings, A. Bergel, B. Erable, Oxygen-reducing biocathodes designed with pure cultures of microbial strains isolated from seawater biofilms, *Int. Biodeterior. Biodegrad.* 103 (2015) 16–22.
- [43] S. Bajracharya, A. ter Heijne, X. Dominguez Benetton, K. Vanbroekhoven, C.J.N. Buisman, D.P.B.T.B. Strik, D. Pant, Carbon dioxide reduction by mixed and pure cultures in microbial electrosynthesis using an assembly of graphite felt and stainless steel as a cathode, *Bioresour. Technol.* 195 (2015) 14–24.
- [44] S. Cheng, D. Xing, D.F. Call, B.E. Logan, Direct Biological Conversion of Electrical Current

- into Methane by Electromethanogenesis, *Environ. Sci. Technol.* 43 (2009) 3953–3958.
- [45] P.F. Beese-Vasbender, J.-P. Grote, J. Garrelfs, M. Stratmann, K.J.J. Mayrhofer, Selective microbial electrosynthesis of methane by a pure culture of a marine lithoautotrophic archaeon, *Bioelectrochemistry*. 102 (2015) 50–55.
- [46] S.T. Lohner, J.S. Deutzmann, B.E. Logan, J. Leigh, A.M. Spormann, Hydrogenase-independent uptake and metabolism of electrons by the archaeon *Methanococcus maripaludis*, *ISME J.* 8 (2014) 1673–1681.
- [47] K. Sato, H. Kawaguchi, H. Kobayashi, Bio-electrochemical conversion of carbon dioxide to methane in geological storage reservoirs, *Energy Convers. Manag.* 66 (2013) 343–350.
- [48] D.F.R. Doud, L.T. Angenent, Toward Electrosynthesis with Uncoupled Extracellular Electron Uptake and Metabolic Growth: Enhancing Current Uptake with *Rhodospseudomonas palustris*, *Environ. Sci. Technol. Lett.* 1 (2014) 351–355.
- [49] N. Aryal, P.-L. Tremblay, D.M. Lizak, T. Zhang, Performance of different *Sporomusa* species for the microbial electrosynthesis of acetate from carbon dioxide, *Bioresour. Technol.* 233 (2017) 184–190.
- [50] N. Aryal, A. Halder, P.-L. Tremblay, Q. Chi, T. Zhang, Enhanced microbial electrosynthesis with three-dimensional graphene functionalized cathodes fabricated via solvothermal synthesis, *Electrochim. Acta.* 217 (2016) 117–122.
- [51] T. Zhang, H. Nie, T.S. Bain, H. Lu, M. Cui, O.L. Snoeyenbos-West, A.E. Franks, K.P. Nevin, T.P. Russell, D.R. Lovley, Improved cathode materials for microbial electrosynthesis, *Energy Environ. Sci.* 6 (2013) 217–224.

**Table 1** Comparison of the current generation by a pure culture of electrotrophic microorganisms in biocathode-based bioelectrochemical systems.

Microorganism	Maximum Current (A m <sup>-2</sup> )	Applied Potential (V)	Cathode area (cm <sup>2</sup> )	References
<i>A. ferrooxidans</i>	-2.0 <sup>a</sup>	+0.2	<sup>e</sup>	[13]
<i>A. ferrooxidans</i>	-5 <sup>c</sup>	+0.0	11.8	[11]
<i>A. ferrooxidans</i> ATCC 23270 <sup>T</sup>	-1.2	-0.34	3	[12]
<i>A. ferrooxidans</i> ATCC 23270 <sup>T</sup>	<sup>b</sup>	+0.4	3.14	[29]
<i>A. ferrooxidans</i> DSM 14882	-0.505	+0.045	11.85	[41]
<i>Acidithiobacillus thiooxidans</i> DSM 14887	-0.023	-0.5	11.85	[41]
<i>Bacillus</i> sp.	-0.04	-0.3	20	[42]
<i>Clostridium ljungdahlii</i> DSM 13528	-1	-0.9	15	[43]
<i>Clostridium pasteurianum</i> DSM 525	-0.004	-0.5	11.85	[41]
<i>Cupriavidus metallidurans</i> DSM 2839	-0.002	-0.5	11.85	[41]
<i>Cupriavidus necator</i> DSM 13513	-0.001	-0.5	11.85	[41]
<i>Desulfosporosinus orientis</i> DSM 765	-0.041	-0.5	11.85	[41]
<i>Desulfovibrio piger</i> DSM 749	-0.016	-0.5	11.85	[41]
<i>Marinobacter</i> sp.	-0.04	-0.3	20	[42]
<i>Methanobacterium palustre</i> ATCC 1077	-0.07 <sup>d</sup>	-0.7	14	[44]
<i>Methanobacterium</i> -like archaeon IM1	-0.097 <sup>d</sup>	-0.4	13	[45]
<i>Methanococcus maripaludis</i> MM901	-0.286 <sup>d</sup>	-0.7	8	[46]
<i>Methanothermobacter thermautotrophicus</i> ΔH	-0.390 <sup>d</sup>	-1.5	3	[47]
<i>Pseudoalteromonas</i> sp.	-0.8	-0.6	20	[42]
<i>Rhodopseudomonas palustris</i> TIE-1	-0.005	-0.220	81	[48]
<i>Roseobacter</i> sp.	-0.035	-0.3	20	[42]
<i>S. acidovorans</i> DSM 3132	-0.572	-0.69	36	[49]
<i>S. aerivorans</i> DSM 13326	-0.026	-0.69	36	[49]
<i>S. malonica</i> DSM 5090	-0.703	-0.69	36	[49]
<i>S. ovata</i> DSM 2662	-2.45	-0.69	22.5	[50]
<i>S. ovata</i> DSM 2663	-0.782	-0.69	36	[49]
<i>S. ovata</i> DSM 3300	-0.191	-0.69	36	[49]
<i>Sporomusa ovata</i> DSM 2662	-0.475 <sup>d</sup>	-0.6	47	[51]
<i>Sulfurimonas denitrificans</i> DSM 1251	-0.021	-0.5	11.85	[41]
<i>Thioalkalivibrio nitratreducens</i> DSM 14787	-0.62	-0.3	6	[27]
<i>Thiobacillus denitrificans</i> DSM 12475	-0.023	-0.5	11.85	[41]
<i>A. ferrooxidans</i> ATCC 23270 <sup>T</sup>	-38.61	-0.2	3	This study

<sup>a</sup>Sustained current density; <sup>b</sup>≈ -6 to -7 μA m<sup>-2</sup>; <sup>c</sup>CV based current density; <sup>d</sup>Average current density; <sup>e</sup>Not mentioned.

## Figure legends

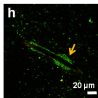
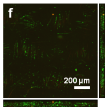
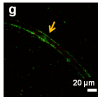
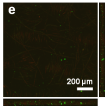
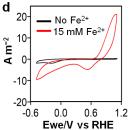
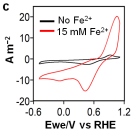
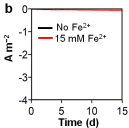
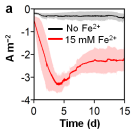
**Fig. 1** Current formation from the biocathodes developed with a pure culture of *A. ferrooxidans*. (a) Biotic and (b) abiotic current density patterns in the absence and presence of  $\text{Fe}^{2+}$  ions in the 9K medium and the data are shown as the mean  $\pm$  SD ( $n = 3$ ). (c) Biotic and (d) abiotic CVs in the absence and presence of 15 mM  $\text{Fe}^{2+}$  ions. (e & f) CLSM 3D projection (Z-stack) micrographs of the biofilms in the absence and presence of 15 mM  $\text{Fe}^{2+}$  ions, respectively. The top layer of the biofilm and related projections are shown in the  $x$  (bottom) and  $y$  (right) axis. (g & h) CLSM micrographs of the biofilm on the single carbon fiber (yellow arrow) in the absence and presence of 15 mM  $\text{Fe}^{2+}$  ions, respectively.

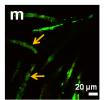
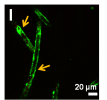
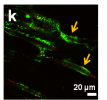
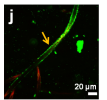
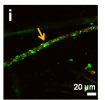
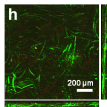
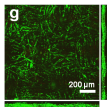
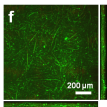
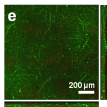
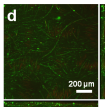
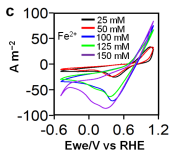
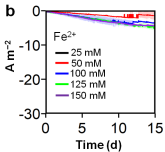
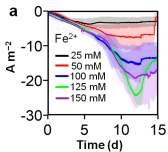
**Fig. 2** Effect of  $\text{Fe}^{2+}$  ion concentration on biocathode development with *A. ferrooxidans* and current generation. (a) Biotic and (b) abiotic current density patterns with the different initial concentrations of  $\text{Fe}^{2+}$  ions (25, 50, 100, 125, and 150 mM) in the 9K medium and the data are shown as the mean  $\pm$  SD ( $n = 3$ ). (c) CVs were recorded from the biocathodes with different concentrations of  $\text{Fe}^{2+}$  ions. (d, e, f, g & h) CLSM 3D projection (Z-stack) micrographs of the cathode biofilms obtained from biotic reactors supplemented with 25, 50, 100, 125, and 150 mM  $\text{Fe}^{2+}$  ions, respectively. The top layer of the biofilm and related projections are shown in the  $x$  (bottom) and  $y$  (right) axis. (i, j, k, l & m) CLSM micrographs of the biofilm on the single carbon fiber (yellow arrow) in the presence of 25, 50, 100, 125, and 150 mM  $\text{Fe}^{2+}$  ions, respectively.

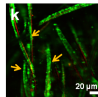
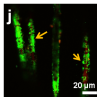
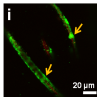
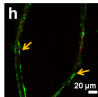
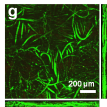
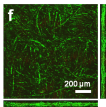
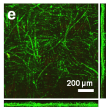
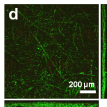
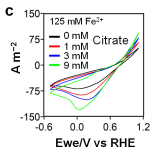
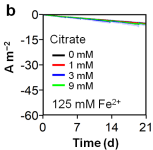
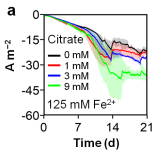
**Fig. 3** Effect of iron chelator (citrate) concentration on biocathode development with *A. ferrooxidans* and current generation. (a) Biotic and (b) abiotic current density recorded from the reactors with 9K1 electrolyte medium plus 125 mM  $\text{Fe}^{2+}$  ions and different concentrations of citrate (0, 1, 3, and 9 mM and the data are shown as the mean  $\pm$  SD ( $n = 3$ ). (c) CVs were recorded from the biocathodes with different concentrations of citrate. (d, e, f & g) CLSM images (Z-stack) of the cathodic biofilms obtained from the biotic reactors supplemented with 0, 1, 3, and 9 mM citrate, respectively (scale bar, 200  $\mu\text{m}$ ). The top layer of the biofilm and related projections are shown in the  $x$  (bottom) and  $y$  (right) axis. (h, i, j & k) CLSM micrographs of the biofilm on the single carbon fiber (yellow arrow) in the presence of 125 mM  $\text{Fe}^{2+}$  medium supplemented with 0, 1, 3, and 9 mM citrate, respectively.

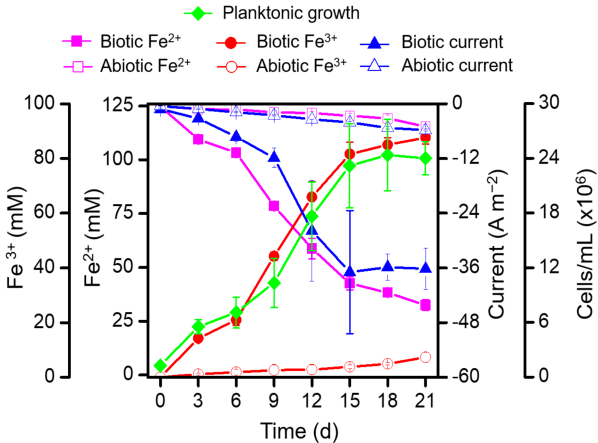
**Fig. 4** The growth curve, iron oxidation/reduction, and current production by *A. ferrooxidans* vs. time. 9K1 medium consist of 125 mM Fe<sup>2+</sup> and 9 mM citrate along with poised potential -0.2 V vs. Ag/AgCl for 21 days at 30 °C. Fe<sup>2+</sup>, Fe<sup>3+</sup>, current density, and bacterial cell count were determined from the samples drawn from the reactors at the three-day interval. The data are shown as the mean ± SD (*n* = 3).

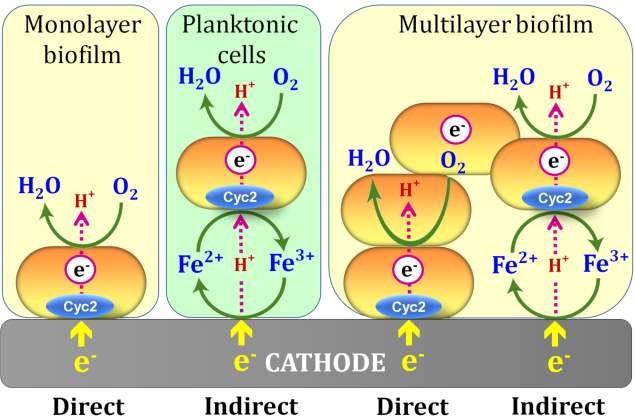
**Fig. 5** Schematic representation of the possible electron transfer mechanisms involved in *A. ferrooxidans* during electrochemical cultivation. *A. ferrooxidans* develop mono and multi-layer biofilm in the absence and presence of iron and could possibly perform direct and indirect electron transfer mechanisms, respectively.



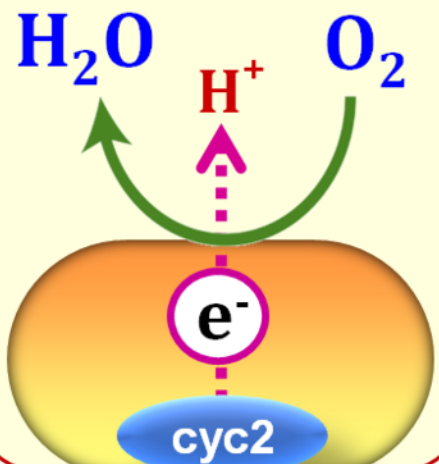








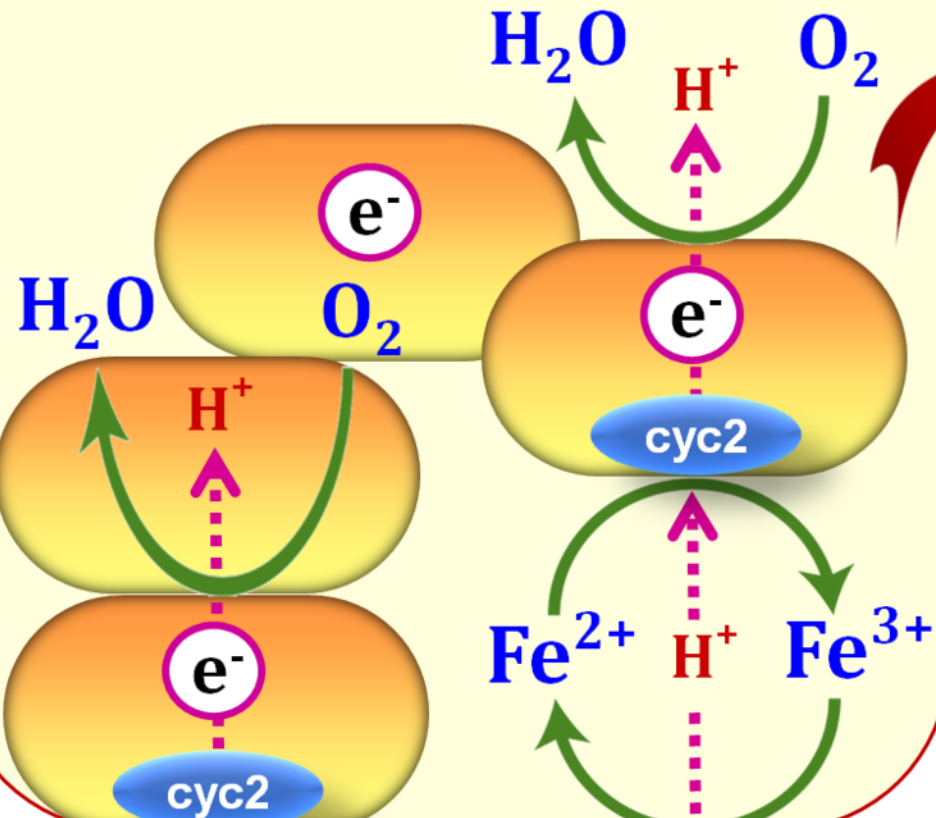
## Monolayer biofilm



$\uparrow$   
 $\text{e}^-$

Direct

## Multilayer biofilm



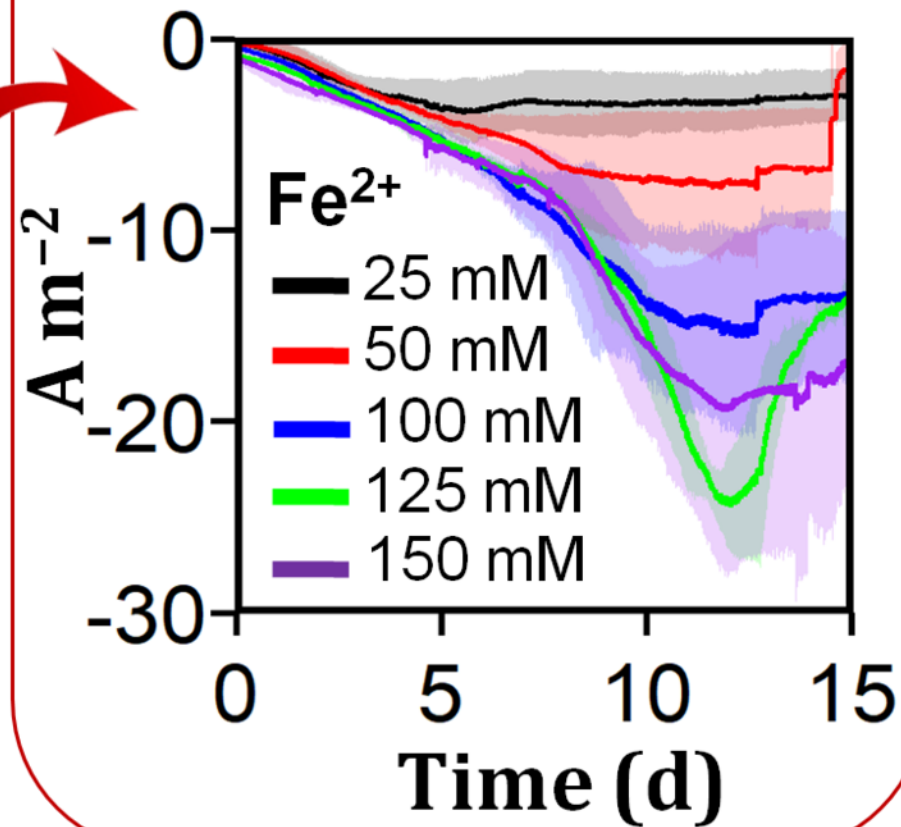
$\uparrow$   
 $\text{e}^-$

Direct

$\uparrow$   
 $\text{e}^-$

Indirect

## Current Generation



*Acidithiobacillus ferrooxidans*  
BIOCATHODE